Correlations between osteocalcin content, degree of mineralization, and mechanical properties of *C. Carpio* rib bone

M. E. Roy,[1] S. K. Nishimoto,[2] J. Y. Rho,[1] S. K. Bhattacharya,[3] J. S. Lin,[4] G. M. Pharr[5,6]
[1]*Department of Biomedical Engineering, The University of Memphis, Memphis, TN*
[2]*Department of Biochemistry, The University of Tennessee, Memphis, TN*
[3]*Department of Surgery, The University of Tennessee, Memphis, TN*
[4]*Solid State Division, Oak Ridge National Laboratory, Oak Ridge, TN*
[5]*Department of Materials Science, The University of Tennessee, Knoxville, TN*
[6]*Metals and Ceramics Division, Oak Ridge National Laboratory, Oak Ridge, TN*

Received 13 March 2000; accepted 17 July 2000

Abstract: Osteocalcin is one of the most abundant noncollagenous proteins in bone. It is strongly associated with the mineral phase of bone, and has long been associated as a marker of bone turnover. However, its relationship to bone composition, strength, and structure is unclear. Carp rib bone is an excellent model for the study, because osteocalcin represents almost 60% of the total extractable noncollagenous proteins found in it. Because of the abundance of osteocalcin relative to other extractable proteins, any changes in the properties of carp rib bone would be more likely influenced by the osteocalcin concentration. To test the hypotheses that the concentration of osteocalcin is reflected in other properties of bone, the correlations between the osteocalcin concentration and the mineral content, microstructural properties, and physical characteristics of the bone mineral crystals were determined utilizing radioimmunoassay (RIA), spectrophotometry, nanoindentation, and small-angle X-ray scattering (SAXS) techniques, respectively. Osteocalcin concentration was found to be correlated to the molar Ca/P ratio and inversely correlated to the elastic modulus and hardness in the longitudinal plane. This study provides evidence for a putative relationship between the concentration of osteocalcin and the microstructural mechanical properties of bone. Correlations were also found between the mechanical properties in the longitudinal plane and both the phosphate content and the molar Ca/P ratio. However, no relationships could be identified between osteocalcin concentration and several parameters of bone crystals, as determined by SAXS. © 2000 John Wiley & Sons, Inc. J Biomed Mater Res 54: 547–553, 2001

Key words: osteocalcin; mineralization; nanoindentation; small-angle X-ray scattering; bone elasticity

INTRODUCTION

Osteocalcin (OC), also known as γ-carboxyglutamic acid-containing protein (BGP), is one of the most extensively studied and most abundant noncollagenous proteins found in bone matrix. It has a strong affinity for hydroxyapatite (HA) but not for amorphous calcium phosphate, and is a potent inhibitor of HA formation.[1] Osteocalcin is a biochemical marker of bone metabolism or turnover,[2] but its precise pathophysiologic role still remains unclear. In developing bone, an increase in osteocalcin concentration closely follows the mineralization phase, suggesting that its informational function is to regulate bone turnover.[3] Osteocalcin is thought to function as a signal in the formation, recruitment, differentiation, and/or activation of bone-resorbing osteoclasts.[4,5]

Osteocalcin deficiency has long been associated with increased bone formation,[6,7] but with little effect on morphology or structure.[8] OC expression is restricted to growing bone (or bone to be mineralized), implicating its role in the modulation or mineralization of bone.[9] OC-deficient transgenic mice have in-

Correspondence to: Jae-Young Rho, Ph.D., Department of Biomedical Engineering, The University of Memphis, Campus Box 526582, Memphis, TN 38152–6582; e-mail: jrho@cc.memphis.edu

Contract grant sponsor: Whitaker Foundation
Contract grant sponsor: UT-CAN-DO Laboratory research fund
Contract grant sponsor: NIH; contract grant numbers: AR45297; R01AR-38540
Contract grant sponsor: U.S. Department of Energy; contract grant number: DEAC0596OR22464
Contract grant sponsor: SHaRE Program; contract grant number: DEAC0576OR00033

© 2000 John Wiley & Sons, Inc.

creased bone formation without impairing bone resorption or affecting mineral content, suggesting osteocalcin prevents excessive bone formation.[10] However, studies to determine the relationship between OC concentration and mechanical properties have been inconclusive; OC-deficient mouse bones tested in 4-point bending exhibited a significantly higher failure load relative to wild-type mice, but no differences in yield energy and stiffness were found.[10] A significant positive correlation between OC concentration and the molar Ca/P ratio has also been reported.[11] Review of the literature to examine the potential effects of osteocalcin on the mineral content of bone have shown no correlation,[8,10,12] an inverse correlation,[13] or mixed results.[14] The reasons for these discrepancies are unknown, but each study measured mineral content in different ways.

The hypotheses of the current study are that the distribution of osteocalcin concentration is reflected in the following properties: molar Ca/P ratio (an indicator of the degree of mineralization present); the microstructural mechanical properties in the transverse and longitudinal planes; and several physical properties of the mineral crystals that comprise bone. Several studies in the literature attempt to correlate OC concentration in serum or in bone with an index of the degree of mineralization of bone. However, at the time this study began, only one report had been published examining the relationship between OC content and mechanical properties,[10] and none investigating the influence of OC concentration on the physical characteristics of bone mineral crystals. The results of this study should help characterize the role of OC in determining the mineralization, the microstructural mechanical properties, and the crystal properties of bone.

METHODS

The first through fifth pairs of ribs were harvested from a fresh frozen 9 lb carp (*Cyprinus carpio*). A carp rib bone model was chosen for study primarily because of its unusually high content (~60%) of OC relative to other extractable proteins, similar to bluegill rib bone,[15] and the existence of an RIA for carp OC. Because of the abundance of OC relative to other extractable proteins in carp rib bone, any changes in the properties of bone would be more likely due to the concentration of osteocalcin present, effectively amplifying its relative importance. Fish bone can be classified as cellular or acellular, depending on the presence of osteocytes. Cellular fish bone, which includes *C. carpio*,[16] is similar to mammalian bone, but undergoes little internal remodeling and lacks osteons,[17] like rat bone.[18] Subsequent inspections of H & E stained carp rib bone specimens confirmed it was cellular bone (data not shown).

Each of the three pairs of ribs were cut into 14 pieces of approximately 5 mm each, producing segments of bone each representing about 6% of the overall length. The most distal segment of each rib was also left longer, if necessary. Specimens were divided up such that alternating pieces were used for different tests. The end result was seven levels of discretization along the length of the rib for every test.

Specimens used for assays were prepared by extracting their mineral and soluble proteins with 10% formic acid over a period of 24 h, following an established method.[19] Supernatants of the specimen extracts were used in all subsequent assays. The OC content was determined in triplicate by a radioimmunoassay (RIA) for carp osteocalcin. Raw data were normalized to the initial sample weight and corrected for dilution, as described previously.[20]

The degree of mineralization of the bone specimens was determined spectrophotometrically. Phosphate assays were performed in duplicate following Sigma Diagnostics' Procedure 360-UV. Ultra-violet absorbance was read on a SPECTRAmax® *PLUS* (Molecular Devices Corporation, Sunnyvale, CA) spectrophotometer at 340 nm. Calcium was assayed by flame atomic absorption spectroscopy (AAS) using a Varian AA775 AAS (Varian Techtron Pty. Ltd., Springvale, Australia), at a wavelength of 422.7 nm.[21] The Ca/P ratio, an index of the degree of mineralization, was determined upon adjustment for dilution factor and normalization to the initial sample weight.

Microstructural mechanical properties were determined by nanoindentation. Nanoindentation methods are based on Sneddon's solution to the axisymmetric Boussinesq problem,[22] which provided simple formulae relating the depth of penetration of an indenter of arbitrary profile with the applied force required for the indenter to make the impression. Nanoindentation methods were developed from hardness testing methods to determine the properties of thin films[23] and were subsequently refined.[24,25] The material properties of a specimen at the microstructural level can now be determined with a spatial resolution of better than 1 mm.[26,27]

Specimens for nanoindentation were taken from ribs 1, 3, and 5, and prepared by mounting transverse and longitudinal sections of bone in epoxy resin and polishing to a 0.05 mm finish. Specimens were tested using the Nanoindenter® II at the Oak Ridge National Laboratory (ORNL). Each specimen was programmed for at least three indentations with target depths of about 1 mm. The experiments yielded data for indentation modulus (E, a measure of elasticity) and hardness (H, a measure of a material's resistance to penetration by a hard object). The microstructural mechanical properties were determined from indentations in the transverse (T) and longitudinal (L) planes, with Poisson's ratio assumed to be 0.3. Figure 1(A) illustrates the transverse and longitudinal planes examined in this study.

Small-angle X-ray scattering (SAXS) methods allow the determination of the physical properties of the inhomogeneities within materials under investigation. A crystal diffracts an incident X-ray beam at specific angles depending on the wavelength of the X-ray, the crystal orientation, and the structure of the crystal.[28] Conceptually, SAXS is similar to the scattering of visible light in an inhomogeneous material. The scattering of light originates from differences in the refractive index of the neighboring phases, while SAXS results from the differences in the electron density in heterogeneous microstructures.[29,30] In a typical SAXS measurement, a beam of highly collimated X-rays is focused incident

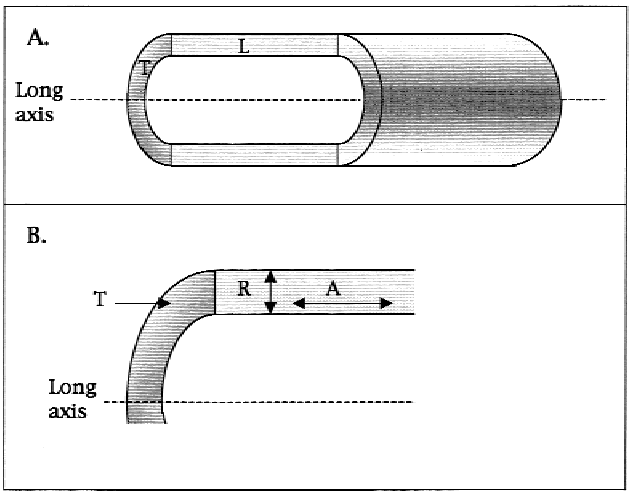

Figure 1. (A) Sketch of a typical section of a carp rib bone, which can be represented as a gently curving, hollow cylinder, illustrating the orientations of interest: (A) axial direction, (T) transverse, and (L) longitudinal planes. (B) Close-up, to show detail for SAXS specimens. Within the longitudinal plane there are two directions: the (A) axial direction and the (R) radial direction.

to a specimen (gas, liquid, or solid). The scattered radiation of the X-rays due to the inhomogeneities in the specimen is measured, typically with a two-dimensional position-sensitive X-ray proportional detector. To probe a specimen microstructure ranging from a few Ångstroms to hundreds of Ångstroms, the scattering angle must be small. In addition, the detector must be positioned several meters away from the sample under investigation to achieve the requisite resolution.

Experimentally, raw data from the SAXS measurements were collected by the 64 × 64 two-dimensional virtual pixel array of the detector via a data acquisition computer. The counts stored in the memory were displayed in a two-dimensional contour plot showing the angular distribution of scattered X-ray photons in isotropic or anisotropic scattering. For each specimen, the scattering momentum transfer function Q and the scattering intensity $I(Q)$ were calculated based on the scattering configuration geometry and instrumental resolution. The transfer function is defined as $Q = (4\pi/\lambda)\sin(\theta/2)$, where λ is the X-ray wavelength and θ is the scattering angle. The scattering intensity $I(Q)$ is defined as the total number of X-ray photons scattered in the direction defined by Q per unit area.[31] The scattering contour plot is generally circular in shape, but it can be a variety of patterns depending the formation, orientation, and morphology of microstructures within materials. A typical case is where the scatterer is exceedingly thin in one dimension, causing the diffraction spots to broaden into lines parallel to that dimension, and resulting in an ellipsoid-shaped contour plot.[32]

The primary scatterers of X-rays in bone are the bone crystals. Raw data from SAXS measurements allow the physical characterization of bone crystals.[33] Physical characteristics that can be determined include periodicity (d, derived from optical theory[34]), average inhomogeneity "grain" size (a[29,30]), power-law scattering "shape function" (α, derived from fractal theory [35,36]), and minimum average dimension (T, relating the volume of a material to its surface area[31,37,35]). SAXS data can be analyzed azimuthally for circular-shaped isotropic scattering patterns, or by sector for anisotropic scattering patterns, with each sector representing one dimension of the scatterers within the specimen. The one-dimensional corrected scattering intensities $I_c(Q)$ were obtained after a proper correction for the sample transmission and thickness, background scattering, dark current, and detector sensitivity corrections.

Specimens for small-angle X-ray scattering were from transverse and longitudinal sections of rib 3 only. After sections were cut, they were mounted individually on a specimen wheel made available at the ORNL SAXS facility. The ORNL 10-m SAXS system was equipped with a Rigaku X-ray rotating anode generator, a pyrolytic graphite monochromator, a 20 × 20 cm two-dimensional position-sensitive detector, and an online data acquisition computer.[38] The X-ray source was Cu K_α radiation (wavelength λ = 1.54 Å), operated at 40 kV and 80 mA. In the current study, data were collected in three dimensions of the samples, from transverse and longitudinal sections of bone, as illustrated in Figure 1: transverse plane (T), and longitudinal plane (L), radial (R), and axial (A) directions (assuming a cylindrical coordinate system).

The parametric, linear independence, or dependence between pairs of variables was determined by computing their parametric correlation coefficient (r). For each correlation test, individual data points for each variable in each section were averaged for comparison. Fisher's Z transformation, with the Hotelling transformation (because $n < 25$), was used to provide p-values. For the SAXS variables, the smaller sample size dictated the use of an alternative test, the Spearman Rank Correlation Coefficient test. In both cases, a positive value of r indicated a positive linear relationship, whereas a negative value indicated an inverse relationship. A significance level of 95% was used for all tests.

RESULTS

A summary of all measurements made in the current study is given in Table I, organized by biochemical measurements, mechanical measurements, and SAXS measurements. A summary of the results of all statistically significant (p = 0.05) correlation tests is given in Table II. The parametric correlation tests revealed a positive linear relationship between OC concentration and molar Ca/P ratio (Table II). Figure 2 shows that the molar Ca/P ratio increased as OC content increased. No statistically significant relationships were found between OC and the concentrations of calcium or phosphate. A significant negative correlation was found between OC concentration and the microstructural elastic modulus (E_L) and hardness (H_L) in the longitudinal plane, but not in the transverse plane (Table II). Figure 3 shows that E_L decreased as OC content increased. No correlations were found between OC concentration and any of the bone crystal parameters, as measured by SAXS.

TABLE I
Summary of (A) the Biochemistry and Nanoindentation Measurements, and (B) the SAXS Measurements Performed in This Study

A. Variable	Plane	Mean ± S.D.	(n)
μg OC/mg bone	—	0.492 ± 0.11	(61)
mg Ca/mg bone	—	0.188 ± 0.0076	(40)
mg PO_4/mg bone	—	0.251 ± 0.020	(40)
molar Ca/P ratio	—	1.79 ± 0.15	(38)
E_T (GPa)	Transverse plane	15.9 ± 1.2	(68)
H_T (GPa)	Transverse plane	0.359 ± 0.062	(68)
E_L (GPa)	Longitudinal plane	8.86 ± 0.74	(58)
H_L (GPa)	Longitudinal plane	0.249 ± 0.025	(58)
B. Variable	**Plane/direction**	**Median (range)**	**(n)**
d_R (nm)	Radial direction	6.58 (1.1)	(7)
a_R (nm)	Radial direction	1.51 (0.12)	(7)
α_R	Radial direction	1.68 (0.40)	(7)
T_R (nm)	Radial direction	1.53 (0.22)	(7)
d_A (nm)	Axial direction	11.1 (4.9)	(7)
a_A (nm)	Axial direction	1.63 (0.46)	(7)
α_A	Axial direction	1.99 (0.47)	(7)
T_A (nm)	Axial direction	1.68 (0.19)	(7)
d_T (nm)	Transverse plane	6.75 (1.3)	(7)
a_T (nm)	Transverse plane	1.19 (0.47)	(7)
α_T	Transverse plane	1.76 (0.40)	(7)
T_T (nm)	Transverse plane	1.80 (0.45)	(7)

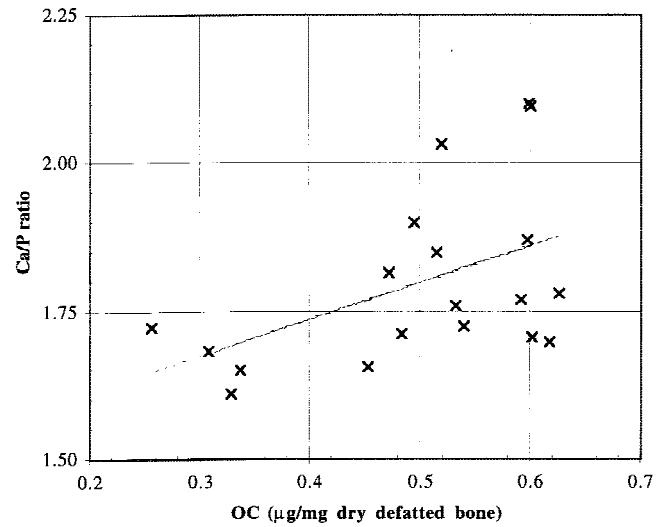

Figure 2. Molar Ca/P ratio as a function of osteocalcin concentration. The data points on the left-hand side of the plot, which included the most distal bone section from all three ribs, also had the generally lowest molar Ca/P ratio by section. The molar Ca/P ratio data were found to be linearly proportional to the amount of OC present (p <0.05), from the correlation coefficient analysis. The dotted line is its linear regression line, with slope = 0.62, intercept = 1.48, and r^2 = 0.24.

Additional correlations were found among the other variables, listed in Table II. Significant correlations were found between E_L and both the phosphate concentration (positive) and the molar Ca/P ratio (inverse). Correlations were also discerned between H_L and Ca/P, and between H_T and PO_4 as well. A total of three inverse correlations were found between SAXS variables and the degree of mineralization and nanoindentation variables (α_T and PO_4; a_A and Ca/P; and α_A and E_T). The correlation between E and H is

TABLE II
Statistically Significant (p < 0.05) Results of the Parametric Correlation Test and the Spearman Rank Correlation Test, Represented by the Sample Correlation Coefficient (r) and Significance of Each Analysis

	Variables			
n[a]	Independent	Dependent	r	Significance
(Parametric correlation coefficient test used)				
19	OC	Ca/P	0.488	p < 0.05
21	OC	E_L	−0.435	p < 0.05
21	OC	H_L	−0.574	p < 0.01
19	PO_4	Ca/P	−0.878	p < 0.0001
20	PO_4	H_T	0.461	p < 0.05
20	PO_4	E_L	0.550	p < 0.05
19	Ca/P	E_L	−0.539	p < 0.05
19	Ca/P	H_L	−0.464	p < 0.05
21	E_T	H_T	0.654	p < 0.001
21	E_L	H_L	0.756	p < 0.001
(Spearman Rank Correlation test used, due to smaller sample size)				
7	PO_4	α_T	−0.811	p < 0.05
6	Ca/P	a_A	−0.943	p < 0.05
7	E_T	α_A	−0.821	p < 0.05

[a]One Ca and one PO_4 specimen were lost during their respective assays, reducing the maximum value of n from 21 to 20 (and 19 for the Ca/P ratio).

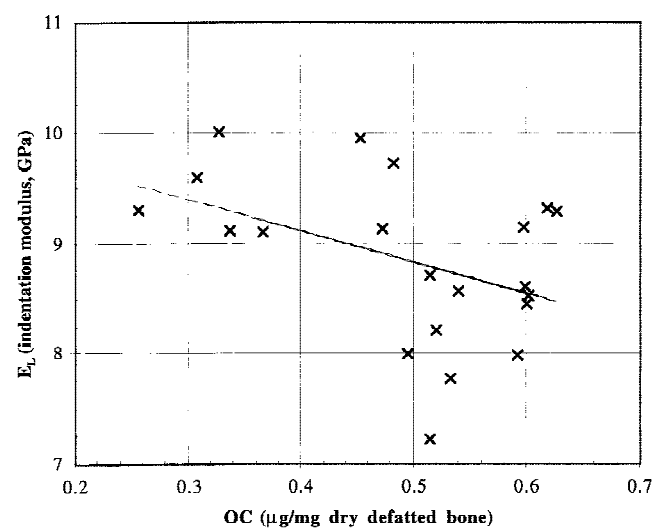

Figure 3. Indentation elastic modulus in the longitudinal direction as a function of osteocalcin concentration. The data points on the left-hand side of the plot, which included the most distal bone section from all three ribs, also had the generally highest indentation modulus by section. The longitudinal elastic modulus data were found to be inversely linearly proportional to the amount of OC present from the correlation coefficient analysis (p < 0.05). The dotted line is its linear regression line, with slope = 2.85, intercept = 10.25, and r^2 = 0.19.

not unusual, occurring in many ceramics and ceramic composites. The inverse correlation between PO_4 concentration and the molar Ca/P ratio was not a surprise, as the latter is a function of the former. However, a similar correlation was not observed between Ca concentration and molar Ca/P ratio.

DISCUSSION

In this study a significant positive correlation was found between the concentration of osteocalcin and the degree of mineralization, as measured by the molar Ca/P ratio (Fig. 2). A similar correlation was found by Boskey et al.,[11] who reported a significant difference between the molar Ca/P ratio of ovariectomized OC-deficient and wild-type mice (Ca/P = 1.26 and 1.41, respectively). In the present study, the measured Ca/P ratios were generally in excess of 1.67, the ratio observed in hydroxyapatite. The lack of correlation between calcium concentration and the molar Ca/P ratio suggests that some Ca is present in a form other than a calcium phosphate. The higher Ca/P ratios may reflect the limited substitution of carbonate for phosphate, as calcium carbonate,[39] in the mineral phases present. This supports the notion that bone is a combination of different mineral phases rather than just a single apatite phase.[40] No significant correlations were found between Ca or PO_4 content and OC concentration.

Significant inverse correlations between OC and the microstructural mechanical properties of bone were found, but only in the longitudinal plane (Fig. 3). Like most long bones, the mechanical properties in the transverse plane were found to be significantly larger than those of the longitudinal plane, but no correlation was found between OC and either E_T or H_T. An inverse correlation between OC concentration and the elastic modulus (measured by compression) of bone has also recently been reported in core samples from the inferior region of the anterior/posterior axis of the human femoral head.[13] However, unlike the current study, the investigators also found an inverse relationship between OC concentration and volumetric bone mineral density, a measure of bone mineralization that should correlate with the molar Ca/P ratio. A previous study on macroscopic specimens found an increase in four-point bending failure load in OC-deficient mice relative to wild-type mice, which was attributed to the increase in bone mass.[10] However, in the current study, the decrease in microstructural elastic modulus with increasing OC concentration indicates that an increase in mineralization (and, hence, bone mass) is not necessarily reflected by an increase in some mechanical properties.

The plane-specificity of the current study may be directly related to a position-specific binding of OC between the inorganic (mineral) and organic (collagen) phase of bone, given the affinity of OC for hydroxyapatite[1] and collagen type I.[41] Alternatively, it may be due to an indirect influence of OC concentration on the mechanical properties, by control of the degree of mineralization. Given the results of the recent femoral head study,[13] which conflict with the latter explanation, it seems likely that there is a direct relationship between osteocalcin concentration and elastic modulus.

No significant physical correlations were found between the concentration of osteocalcin and any of the bone crystal parameters measured (periodicity, average inhomogeneity size, "shape function" exponent, and minimum average dimension). However, a temporal relationship has been suggested by the appearance of osteocalcin about two weeks after the deposition of bone mineral.[3] Indeed, Hunter et al.[12] subsequently found that osteocalcin inhibited hydroxyapatite crystal formation by delaying nucleation rather than altering the amount of hydroxyapatite formed.

The scattering exponent in the transverse plane (α_T) was found to be inversely proportional to the phosphate concentration ($p < 0.05$). It is generally agreed that mature bone is composed of plateshaped crystals[42] with $\alpha = 2$, whereas immature bone composed of needle-shaped crystals has $\alpha = 1$.[36] This correlation implies that the bone crystals are more plateshaped when the amount of phosphate is lower.

An inverse relationship was also found between minimum average inhomogeneity size (a_A) and the molar Ca/P ratio ($p < 0.05$). The correlation suggests that the bone crystals become smaller as Ca/P ratios exceed the ideal 1.67 ratio for hydroxyapatite.

Lastly, the scattering shape function in the longitudinal plane, axial direction (α_A) was found to be inversely proportional ($p < 0.05$) to the elastic modulus in the transverse plane (E_T). This study found α_A to be generally around 2, implying that the bone crystals found in the carp rib bone tested are plate-shaped. The correlation found then suggests that as bone crystals mature and become more plate-shaped, the elastic modulus of the resulting bone decreases in the transverse direction.

This study was limited to one specimen of *C. carpio*. A single specimen eliminated the effects of age and sex. The purpose of this study was to test the hypotheses that variations in OC concentration would correlate with changes in various bone properties. Given its unusually large content of OC relative to other extractable proteins, we propose that carp rib bone is an excellent model for examining the importance of osteocalcin in bone.

The results of this study show the concentration of osteocalcin in carp rib bone is correlated to the molar Ca/P ratio as well as to the microstructural mechani-

cal properties in the longitudinal plane only. Phosphate concentration and molar Ca/P ratio were found to be determinants of the elastic properties in the longitudinal plane, but not in the transverse plane. The study provides evidence of a relationship between the concentration of osteocalcin and the microstructural mechanical properties of bone. Although OC comprises almost 60% of the total extractable protein in carp rib bone, the contributions of other proteins in the matrix to mineralization precludes definitive conclusions of the relationship between OC and microstructural mechanical properties.

Portions of this research were sponsored by the Whitaker Foundation and NIH grant #AR45297 (JYR). The AAS facilities at the Surgical Research Laboratories of The University of Tennessee, Memphis was supported in part by grants to SKB from NIH (#R01AR-38540) and the UT-CAN-DO Laboratory research fund. Analytical instrumentation for nanoindentation and small-angle X-ray scattering testing was provided by the Division of Materials Sciences, U.S. Department of Energy, under contract DEAC0596OR22464 with Lockheed Martin Energy Research Corp. and through the SHaRE Program under contract DEAC0576OR00033 between the U.S. Department of Energy and Oak Ridge Associated Universities.

References

1. Price PA, Otsuka AS, Poser JW, Kristaponis J, Raman N. Characterization of a γ-carboxyglutamic acid-containing protein from bone. Proc Natl Acad Sci USA 1976;73:1447–1451.
2. Price PA, Parthemore JG, Deftos LJ. A new biochemical marker for bone metabolism: measurement by radioimmunoassay of bone Gla protein in the plasma of normal subjects and patients with bone disease. J Clin Invest 1980;66:878–883.
3. Price PA, Lothringer JW, Baukol SA, Reddi AH. Developmental appearance of the Vitamin K-dependent protein of bone during calcification. J Biol Chem 1981;256:3781–3784.
4. Malone JD, Teitelbaum SL, Griffin GL, Senior RM, Kahn AJ. Recruitment of osteoclast precursors by purified bone matrix constituents. J Cell Biol 1982;92:227–230.
5. Mundy GR, Poser JW. Chemotactic activity of the γ-carboxyglutamic acid-containing protein in bone. Calcif Tissue Int 1983;35:164–168.
6. Hauschka PV, Lian JB, Gallop PM. Vitamin K and mineralization. Trends Biochem Sci 1978;3:75–78.
7. Price PA, Lothringer JW, Nishimoto SK. Absence of the Vitamin K-dependent bone protein in fetal rat mineral. Evidence for another γ-carboxyglutamic acid-containing component in bone. J Biol Chem 1980;255:2938–2942.
8. Price PA, Williamson MK. Effects of warfarin on bone: studies on the Vitamin K-dependent bone protein on rat bone. J Biol Chem 1981;256:12754–12759.
9. Young MF, Kerr JM, Ibaraki K, Heegaard AM, Robey PG. Structure, expression, and regulation of the major noncollagenous matrix proteins of bone. Clin Orthop Rel Res 1992;281: 275–294.
10. Ducy P, Desbois C, Boyce B, Pinero G, Story B, Dunstan C, Smith E, Bonadio J, Goldstein S, Gundberg C, Bradley A, Karsenty G. Increased bone formation in osteocalcin-deficient mice. Nature 1996;382:448–452.
11. Boskey AL, Gadaleta S, Gundberg C, Doty SB, Ducy P, Karsenty G. Fourier transform infrared microspectroscopic analysis of bones of osteocalcin-deficient mice provides insight into the function of osteocalcin. Bone 1998;23:187–196.
12. Hunter GK, Hauschka PV, Poole AR, Rosenberg LC, Goldberg HA. Nucleation and inhibition of hydroxyapatite formation by mineralized tissue proteins. Biochem 1996;J 317:5964.
13. Brown SJ, Powell DE, Pollintine P, Davie MWJ, Sharp CA. Bone matrix changes in osteoarthritic bone. J Bone Mineral Res 1999;14:S327.
14. Minisola S, Rosso R, Romagnoli E, D'Erasmo E, Manfredi G, Damiani C, De Antoni F, Mazzuoli G. Serum osteocalcin and bone mineral density at various skeletal sites: a study performed with three different assays. J Lab Clin Med 1997;129: 422–429.
15. Nishimoto SK, Padilla SM, Snyder DL. The effect of food restriction and germ-free environment on age-related changes in bone matrix. J Gerontol 1990;45:B164–B168.
16. Moss ML. Studies of the acellular bone of teleost fish. I. Morphological and systematic variations. Acta Anat 1961;46:343–462.
17. Weiss RE, Watabe N. Studies on the biology of fish bone. III. Ultrastructure of osteogenesis and resorption in osteocytic (cellular) and anosteocytic (acellular) bones. Calcif Tissue Int 1979; 28:43–56.
18. Weiner S, Arad T, Traub W. Letter: crystal organization in rat bone lamellae. FEBS 1991;285:49–54.
19. Nishimoto SK, Chang CH, Gendler E, Stryker WF, Nimni ME. The effect of aging on bone formation in rats: biochemical and histological evidence for decreased bone formation capacity. Calcif Tissue Int 1985;37:617–624.
20. Nishimoto SK, Araki N, Robinson FD, Waite JH. Discovery of bone g-carboxyglutamic acid protein in mineralized scales. J Biol Chem 1992;267:11600–11605.
21. Bhattacharya SK, Williams JC, Palmieri GMA. Determination of calcium and magnesium in cardiac and skeletal muscle by atomic absorption spectroscopy using stoichiometric nitrous oxide-acetylene flame. Analyt Lett 1979;12:1451–1475.
22. Sneddon IN. The relation between load and penetration in the axisymmetric Boussinesq problem for a punch of arbitrary profile. Int J Eng Sci 1965;3:47–57.
23. Doerner MF, Nix WD. A method for determining the data from depth-sensing indentation instruments. J Mater Res 1986;1: 601–609.
24. Oliver WC, Pharr GM. An improved technique for determining hardness and elastic modulus using load and displacement sensing indentation systems. J Mater Res 1992;7:1564–1583.
25. Pharr GM, Oliver WC, Brotzen FR. On the generality of the relationship among contact stiffness, contact area, and elastic modulus during nanoindentation. J Mater Res 1992;7:613–617.
26. Pharr GM. Measurement of mechanical properties by ultra-low load indentation. Mater Sci Eng 1998;A253:151–159.
27. Rho JY, Zioupos P, Currey JD, Pharr GM. Variations in the individual thick lamellar properties within osteons by nanoindentation. Bone 1999;25:295–300.
28. Wilson AJC. Elements of X-ray crystallography. Reading: Addison–Wesley; 1970.
29. Debye P, Bueche AM. Scattering by an inhomogeneous solid. J Appl Phys 1949;20:518–525.
30. Debye P, Anderson HR Jr, Brumberger H. Scattering by an inhomogeneous solid. II. The correlation function and its application. J Appl Phys 1957;28:679–683.
31. Fratzl P, Roschger P, Eschberger J, Abendroth B, Klaushofer K. Abnormal bone mineralization after fluoride treatment in osteoporosis: a small-angle X-ray scattering study. J Bone Mineral Res 1994;9:1541–1549.
32. Azároff LV, Kaplow R, Kato N, Weiss RJ, Wilson AJC, Young RA. X-ray diffraction. New York: McGraw–Hill; 1974.
33. Roy ME. The role of osteocalcin in the degree of mineralization,

mechanical properties, and crystal structure of carp rib bone. Ph.D. Dissertation. U Memphis, Memphis, TN; 1999.
34. Bragg SL. The development of X-ray analysis. Phillips DC, Lipson H, editors. London: Bell; 1975.
35. Fratzl P, Fratzl–Zelman N, Klaushofer K, Vogl G, Koller K. Nucleation and growth of mineral crystals in bone studied by small-angle X-ray scattering. Calcif Tissue Int 1991;48:407–413.
36. Schmidt PW. Small-angle scattering studies of disordered, porous, and fractal systems. J Appl Cryst 1991;24:414–435.
37. Brumberger H. Determination of specific surfaces by small-angle X-ray scattering methods — a brief review. van Olphen H, Parrish W, editors. X-ray and electron methods of analysis. New York: Plenum; 1968.
38. Wignall GD, Lin JS, Spooner S. Reduction of parasitic scattering in small-angle X-ray scattering by a three-pinhole collimating system. J Appl Cryst 1990;23:241–245.
39. Nelson DG, Featherstone JD. Preparation, analysis, and characterization of carbonated apatites. Calcif Tissue Int 1982;34: S69–S81.
40. Driessens FCM, Verbeeck RMH. The dynamics of bone mineral in some vertebrates. Z Naturforsch 1986;41c:468–471.
41. Prigodich RV, Vesely MR. Characterization of the complex between bovine osteocalcin and type I collagen. Arch Biochem Biophys 1997;345:339–341.
42. Weiner S, Traub W. Bone structure: from Ångstroms to microns. FASEB J 1992;6:879–885.